Bioorganic Chemistry 86 (2019) 137–150

Contents lists available at ScienceDirect

Bioorganic Chemistry

journal homepage: www.elsevier.com/locate/bioorg

Hydroxyl alkyl ammonium ionic liquid assisted green and one-pot regioselective access to functionalized pyrazolodihydropyridine core and their pharmacological evaluation

Divyang M. Patel[a], Mayank G. Sharma[a], Ruturajsinh M. Vala[a], Irene Lagunes[b], Adrián Puerta[b], José M. Padrón[b], Dhanji P. Rajani[c], Hitendra M. Patel[a,*]

[a] Department of Chemistry, Sardar Patel University, Vallabh Vidyanagar 388120, Gujarat, India
[b] BioLab, Instituto Universitario de Bio-Orgánica Antonio González, CIBICAN, Universidad de La Laguna, Avda. Astrofísico Francisco Sánchez 2, 38206 La Laguna, Spain
[c] Microcare Laboratory and Tuberculosis Diagnosis & Research Center, Surat, India

ARTICLE INFO

Keywords:
Ambiphilic behavior
Cost-effective
E-factor
Environmentally benign
Hydroxyl alkyl ammonium ionic liquids
Pyrazolodihydropyridine
Recyclable
Task-specific

ABSTRACT

Herein our team explored a promising synthetic trail to Functionalized pyrazolodihydropyridine core using hydroxyl alkyl ammonium ionic liquid via one-pot fusion of 3-methyl-1-phenyl-1H-pyrazole-5-amine, different heterocyclic aldehydes and 1, 3-Cyclic diones. The aimed compounds were obtained by Domino-Knoevenagel condensation and Michael addition followed by cyclization. The reaction transformation involves the formation of two C—C and one C—N bond formation. The perspective of the present work is selectively approached to Functionalized pyrazolodihydropyridine core excluding other potential parallel reactions under environmentally benign reaction condition. The present protocol show features such as the low E-factor, ambiphilic behavior of ionic liquid during reaction transformation, scale-up to a multigram scale, reusability of the ionic liquid, mild reaction condition, and produce water as a byproduct. All newly derived compounds were evaluated for their *in vitro* biological activities. In preliminary biological studies compound, **4c** showed better potency than the standard drug ampicillin against Gram-negative bacteria (*E. coli*); the compound **4i** exhibited outstanding activity against *S. aeruginosa* which is far better than ampicillin, chloramphenicol, and ciprofloxacin. The compound **4m** was found more potent against *C. albicans*, than that of griseofulvin and show equipotency to nystatin whereas, in preliminary antitubercular screening, compound **4o** was exhibited more potency than rifampicin. Noteworthy compounds **4f** and **4i** were found most active in antiproliferative screening.

1. Introduction

Multi-component reactions (MCRs) are the powerful tool for convenient synthesis of biologically active scaffolds [1–4]. MCRs facilitate single step conversion over the stepwise conversation of the organic molecules [5–7]. In synthetic chemistry, MCRs proved as ideal synthetic tools for the construction of complex molecule targets because of their inherent convergence power, ease of operation, atom-economy, men power reduction and resource effectivity from the sustainability point of view. The literature survey reveals some pioneering work for the syntheses of pyrazole fused polyheterocyclic compounds. [8–10] Noteworthy, pyrazole fused N-heterocyclic derivatives exhibit potent biological activity and some of them are celecoxib, sildenafil etc. [11–13] pyrazolodihydropyridine and pyrazolopyridine have been studies for antileishmanial activity and found to be potent as an adjunct therapy with miltefosine [14]. Some pyrazole bearing biologically active molecules are shown in Fig. 1.

These basic features of pyrazole bearing moieties attract the researchers for development of the reaction methodology for pyrazolodihydropyridine core. As MCRs involving three or more components, there are molecular interactions between components this sometimes generate the issue of selectivity which leads to other potent parallel reactions [15,16]. Earlier reported protocols for the synthesis of pyrazolo fused dihydropyridines was carried out using triethylamine under microwave irradiation (see ref [9]), imidazolium salts [17] polyethyleneglycol [18], amino acid [19] glacial acetic acid [20] and sodium-1-dodecanesulfonate [21] catalyzed access to pyrazolodihydropyridine derivatives. However, earlier reported protocols faced drawbacks like the use of the expensive, hazardous, non-recoverable catalyst, harsh reaction condition, relatively lower product yield, and

* Corresponding author.
E-mail address: hm_patel@spuvvn.edu (H.M. Patel).

https://doi.org/10.1016/j.bioorg.2019.01.029
Received 31 August 2018; Received in revised form 25 December 2018; Accepted 17 January 2019
Available online 19 January 2019

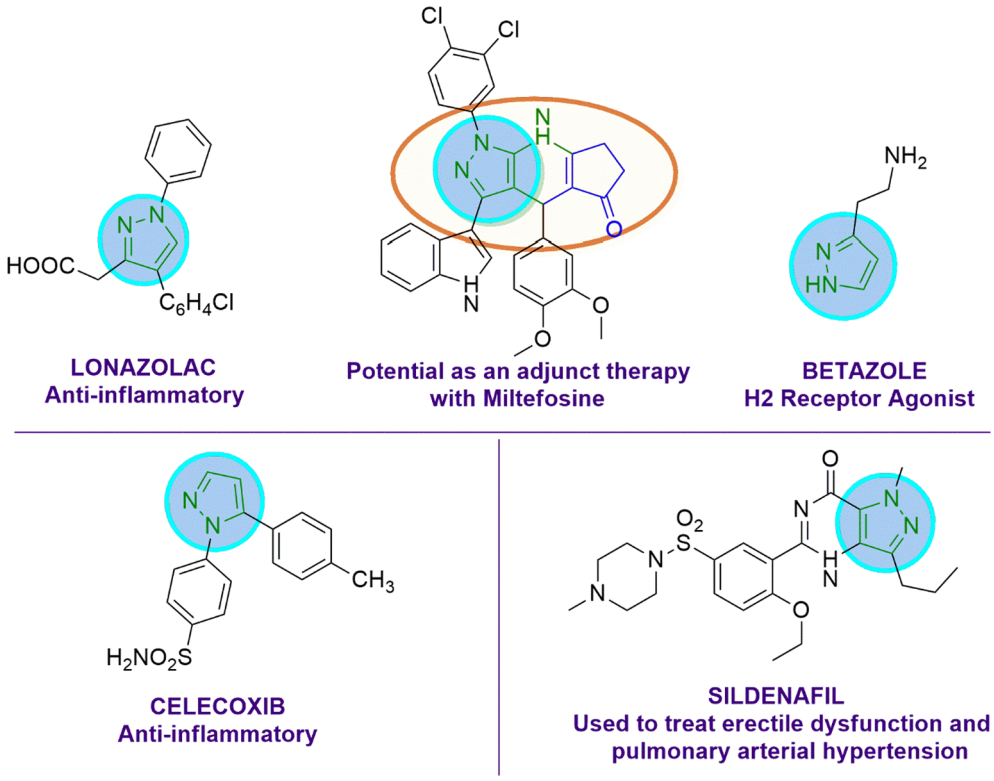

Fig. 1. Some biologically active molecules having pyrazole as a basic constituent.

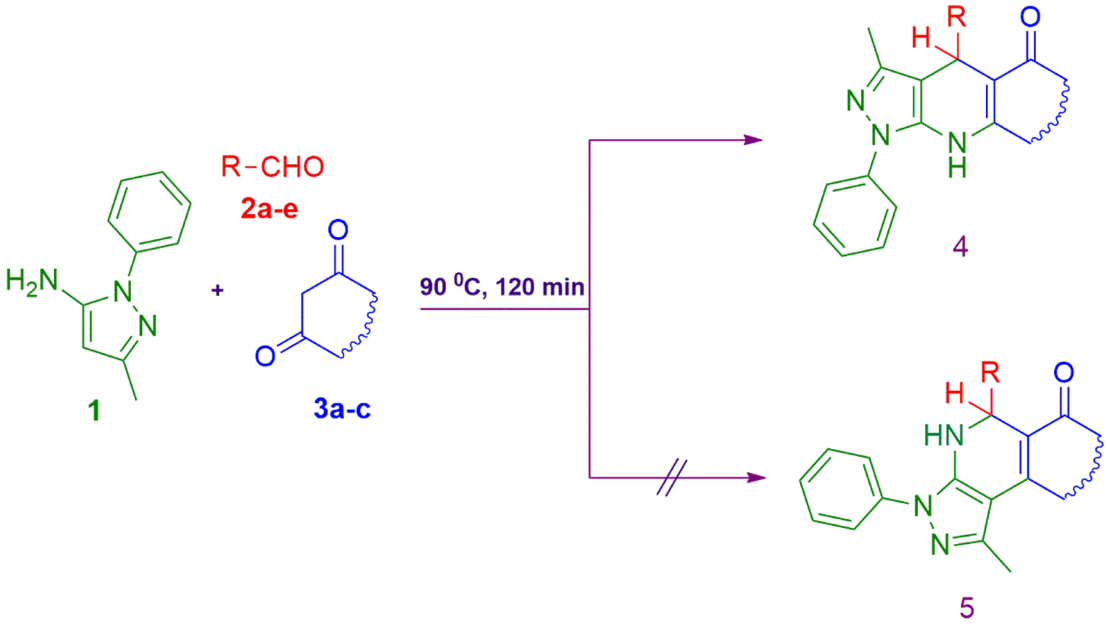

Scheme 1. Ionic liquid triggered selective one-pot access to functionalized pyrazolodihydropyridine core.

tedious work up. As per our literature survey is concerned, there is no reported methodology which mainly involved the utilization of cost-effective, low environment factor, ambiphilic catalytic behavior, atom-economic, less toxic and task-specific ionic liquid. Earlier studies on hydroxyl alkyl ammonium ionic liquids show the wide range of applications in organic syntheses [22–30] reclaiming phenolic compounds from low-temperature coal tar [31] mobile phase modifier for reversed-phase liquid chromatography [32] and also used as media for biocatalytic oxidations [33] etc. (See Scheme 1)

Considering the highlighted pharmacological activities of pyrazolodihydropyridine derivatives and in continuation to our work on the development of biologically active heterocyclic scaffolds [34], here we reported hydroxyl alkyl ammonium ionic liquid catalyzed one-pot regioselective synthesis of the functionalized pyrazolodihydropyridine derivatives.

2. Experimental section

2.1. General informations

All chemicals which are used in the present study were purchased from commercially available sources and used without further purification. The purification of all the synthesized compounds was made by the automated flash chromatographic system (YAMAZEN AI-580S) with HI-FLASH silica gel columns (230–400 μm mesh size) using 50% solution of ethyl acetate in petroleum ether (60–80 °C) as a mobile phase. The Mass analysis of all newly synthesized compounds was collected on MS - Agilent 6120 quadrupole. Melting points were determined by open capillary tube method and are uncorrected. ^{1}H NMR and ^{13}C-APT spectral analysis were recorded on BRUKER AVANCE II 400 NMR Spectrometer using $CDCl_3$ and DMSO-d_6 as the solvents. The chemical shifts are expressed in parts per million and coupling constants (*J*) are provided in Hertz.

2.2. Single-crystal X-ray diffraction analysis

The single-crystal X-ray diffraction data of compounds **4b, 4h, 4i,** and **4j** were collected on a Rigaku SCX mini diffractometer using graphite monochromated Mo-Kα radiation at 293 K temperature. The structures were solved by direct methods [35] and expanded using Fourier techniques. Non-hydrogen atoms were refined isotropically and hydrogen atoms were refined using the riding model. All calculations were performed using the Crystal Structure [36] crystallographic software package except for refinement, which was performed using SHELXL-97 [37].

2.3. General procedure for the synthesis of different hydroxyl alkyl ammonium ionic liquids [38]

Hydroxyl alkyl ammonium ionic liquids were derived by neutralization reaction of Ethanolamine derivatives in ethanol with different acid derivatives. For example, here we described the synthetic procedure of 2-hydroxyethyl ammonium acetate ionic liquid: 2-hydroxyethyl amine (3 mmol) was dissolved in 60 mL of absolute alcohol to form a liquid mixture and charged in 500 mL two neck-flask equipped with reflux condenser and dropping funnel and cooled in an ice bath (0–5 °C). Under vigorous stirring the mixture of acetic acid (3 mmol) in 60 mL of absolute ethanol was then added dropwise by means of dropping funnel in the flask about 90 min by maintaining the temperature below 5 °C. The stirring was continued for 24 h. The excess solvent was evaporated under vacuum. The resulting viscous liquid was further used for the syntheses of compounds.

2.4. General procedure for the synthesis of pyrazolodihydropyridine derivatives 4(a-o)

3-methyl-1-phenyl-5-aminopyrazole **1** (3 mmol), heterocyclic aldehyde **2a-e** (3 mmol), 1, 3-cyclic dione **3a-c** (3 mmol), were charged into 50 mL round bottom flask followed by addition of 2 mL of hydroxyl alkyl ammonium ionic liquid. The content is then stirred at 90 °C until the TLC (50% ethyl acetate in petroleum ether (60–80 °C)) reveals the complete consumption of starting materials. After completion of the reaction, the mixture was poured into ice water and filtered off. The filtrate containing IL was then charged in Rota evaporator and recovered by removing excess water under reduced pressure at 60–70 °C and was reused for subsequent reactions. Furthermore, synthesized compounds were purified by Automated Flash chromatographic system using 50% ethyl acetate in petroleum ether (60–80 °C). The characterization detail of all newly synthesized compounds was shown below.

2.5. General procedure for the development of crystal blocks of 4b, 4h, 4i, and 4j

After chromatographic purification of the synthesized compound, the dried and pure compound (~40 mg) was placed in neat and clean crystal developing vessel followed by addition of ~30 mL of methanol-ethanol (1:1, v/v) as a solvent system. This whole solution is warmed for the preparation of the homogeneous solution and then allowed to cool down gently and placed for slowly solvent evaporation.

2.6. Characterizations details of all newly synthesized pyrazolodyhydropyridine derivatives 4(a-o)

2.6.1. 3-methyl-4-(3-methylthiophen-2-yl)-1-phenyl-6,7,8,9-tetrahydro-1H-pyrazolo [3,4-b] quinolin-5(4H)-one. 4a

White solid; melting point: 261–264 °C; R_f = 0.32; ^{1}H NMR (400 MHz, DMSO-d_6) (δ, ppm): 9.60 (s, 1H, NH),7.38–7.56 (m, 5H, ArH), 7.10 (d, *J* = 5.2 Hz, 1H, Thiophene-CH), 6.66 (d, *J* = 5.2 Hz, 1H, Thiophene-CH), 5.32 (s, 1H, CH), 2.53–2.69 (m, 2H, CH_2), 2.30 (s, 3H, CH_3), 2.22 (t, *J* = 6.0 Hz, 2H, CH_2), 1.91 (s, 3H, CH_3), 1.75–1.88 (m, 2H, CH_2); ^{13}C APT (100 MHz, DMSO-d_6) (δ, ppm): 194.62, 152.90, 146.56, 146.46, 138.67, 136.27, 131.25, 129.88, 129.73, 127.32, 123.56, 122.38, 111.36, 104.62, 37.44, 29.35, 27.78, 21.39, 14.12, 12.36; MS (MM-ES + APCI) 374.3 $(M + H)^+$.

2.6.2. 3,7,7-trimethyl-4-(3-methylthiophen-2-yl)-1-phenyl-6,7,8,9-tetrahydro-1H-pyrazolo[3,4-b]quinolin-5(4H)-one. 4b

White solid; melting point: 230–233 °C; R_f = 0.54; ^{1}H NMR (400 MHz, $CDCl_3$) (δ, ppm): 7.30–7.73 (m, 5H, ArH), 6.96 (d, *J* = 4.8 Hz, 1H, Thiophene-CH), 6.66 (d, *J* = 5.2 Hz, 1H, Thiophene-CH), 5.41 (s, 1H, CH), 2.41 (s, 3H, CH_3), 2.33 (d, *J* = 5.2 Hz, 2H, CH), 2.16 (d, *J* = 9.2 Hz, 2H, CH), 2.09 (s, 3H, CH_3), 1.03 (s, 6H, CH_3); ^{13}C APT (100 MHz, $CDCl_3$) (δ, ppm): 195.27, 148.67, 147.47, 145.15, 138.00, 135.14, 131.71, 131.71, 129.79, 129.47, 127.38, 122.98, 121.85, 111.74, 104.89, 50.72, 42.18, 32.46, 29.26, 27.24, 13.95, 12.10; MS (MM-ES + APCI) 402.3 $(M + H)^+$.

2.6.3. 3-methyl-4-(3-methylthiophen-2-yl)-1-phenyl-4,6,7,8-tetrahydrocyclopenta[b] pyrazolo[4,3-e]pyridin-5(1H)-one. 4c

White solid; melting point: 228–231 °C; R_f = 0.28; ^{1}H NMR (400 MHz, DMSO-d_6) (δ, ppm): 9.97 (s, 1H, NH), 7.20–7.35 (m, 5H, ArH), 6.90 (d, *J* = 5.2 Hz, 1H, Thiophene-CH), 6.51 (d, *J* = 5.2 Hz, 1H, Thiophene-CH), 4.97 (s, 1H, CH), 2.46 (t, *J* = 4.0 Hz, 2H, CH_2), 2.35 (t, 2.0 Hz, 2H, CH_2), 2.13 (s, 3H, CH_3), 1.67 (s, 3H, CH_3); ^{13}C APT (100 MHz, $CDCl_3$ + DMSO-d_6) (δ, ppm): 200.23, 165.47, 146.76, 143.70, 137.95, 137.24, 131.60, 129.16, 129.12, 126.70, 123.03, 122.07, 115.30, 103.75, 33.63, 28.33, 24.23, 13.64, 11.77; MS (MM-ES + APCI) 360.2 $(M + H)^+$.

2.6.4. 4-(5-bromothiophen-2-yl)-3-methyl-1-phenyl-6,7,8,9-tetrahydro-1H-pyrazolo [3,4-b] quinolin-5(4H)-one. 4d

Yellowish white solid; melting point: 218–221 °C; R_f = 0.30; ^{1}H NMR (400 MHz, DMSO-d_6) (δ, ppm): 9.61 (s, 1H, NH), 7.35–7.5 (m, 5H, ArH), 6.83 (d, *J* = 3.6 Hz, 1H, Thiophene-CH), 6.54 (d, *J* = 3.6 Hz, 1H, Thiophene-CH), 5.33 (s, 1H, CH), 2.53–2.68 (m, 2H, CH_2), 2.28 (quint, *J* = 4.8 Hz, 2H, CH_2), 2.05 (s, 3H, CH_3), (m, 2H, CH_2); ^{13}C APT (100 MHz, $CDCl_3$ + DMSO-d_6) (δ, ppm): 194.39, 153.76, 153.18, 145.98, 138.03, 136.31, 129.14, 129.01, 126.78, 123.47, 123.20, 109.92, 108.78, 102.28, 36.79, 30.58, 27.28, 20.78, 11.87; MS (MM-ES + APCI) 440.3 $(M + H)^+$.

2.6.5. 4-(5-bromothiophen-2-yl)-3,7,7-trimethyl-1-phenyl-6,7,8,9-tetrahydro-1H-pyrazolo[3,4-b] quinolin-5(4H)-one. 4e

Yellowish white solid; melting point: 184–187 °C; R_f = 0.51; ^{1}H NMR (400 MHz, DMSO-d_6) (δ, ppm): 9.54 (s, 1H, NH), 7.35–7.51 (m, 5H, ArH), 6.85 (d, *J* = 3.6 Hz, 1H, Thiophene-CH), 6.57 (d, *J* = 3.6 Hz,

Fig. 2. Different hydroxyl alkyl ammonium ionic liquids used in this study.

1H, Thiophene-CH), 5.31 (s, 1H, CH), 2.48 (s, 2H, CH_2), 2.13 (m, 2H, CH_2), 2.05 (s, 3H, CH_3), 0.98 (s, 6H, CH_3); ^{13}C APT (100 MHz, $CDCl_3$ + DMSO-d_6) (δ, ppm): 194.05, 153.76, 151.41, 145.98, 138.00, 136.31, 129.14, 129.06, 126.78, 123.47, 123.16, 108.67, 108.58, 102.34, 50.33, 40.60, 31.85, 30.69, 26.86, 11.87; MS (MM-ES + APCI) 466.2$(M + H)^+$.

2.6.6. 4-(5-bromothiophen-2-yl)-3-methyl-1-phenyl-4,6,7,8-tetrahydrocyclopenta[b] pyrazolo[4,3-e]pyridin-5(1H)-one. 4f

White solid; melting point: 222–225 °C; R_f = 0.26; ^{1}H NMR (400 MHz, DMSO-d_6) (δ, ppm): 10.09 (s, 1H, NH), 7.22–7.36 (m, 5H, ArH), 6.71 (d, J = 4.0 Hz, 1H, Thiophene-CH), 6.55 (d, J = 3.6 Hz, 1H, Thiophene-CH), 4.99 (s, 1H, CH), 2.35 (t, J = 1.6 Hz, 2H, CH_2), 2.17 (t, 2.4 Hz, 2H, CH_2), 1.84 (s, 3H, CH_3); ^{13}C APT (100 MHz, $CDCl_3$ + DMSO-d_6) (δ, ppm): 200.32, 166.16, 152.08, 146.67, 137.79, 137.65, 129.17, 126.92, 124.06, 123.21, 120.88, 114.15, 109.20, 102.13, 33.67, 30.37, 24.20, 12.07; MS (MM-ES + APCI) 426.2 $(M + H)^+$.

2.6.7. 4-(6-bromobenzo[d][1,3]dioxol-5-yl)-3-methyl-1-phenyl-6,7,8,9-tetrahydro-1H-pyrazolo [3,4-b] quinolin-5(4H)-one. 4g

White solid; melting point: 255–258 °C; R_f = 0.33; ^{1}H NMR (400 MHz, DMSO-d_6) (δ, ppm): 9.34 (s, 1H, NH), 7.31–7.49 (m, 5H, ArH), 6.88 (s, 1H, CH), 6.61 (s, 1H, CH), 5.89 (s, 2H, CH_2), 5.34 (s, 1H, CH), 2.65 (s, 2H, CH_2), 2.2 (t, J = 4.8 Hz, 2H, CH_2), 1.93 (s, 3H, CH_3) 1.76–1.91 (m, 2H, CH_2). ^{13}C APT (100 MHz, $CDCl_3$ + DMSO-d_6) (δ, ppm): 194.25, 153.33, 153.10, 146.29, 145.95, 138.06, 136.10, 129.00, 128.23, 126.58, 123.15, 121.06, 115.87, 112.09, 103.04, 101.28, 36.99, 31.81, 27.42, 20.96, 12.46; MS (MM-ES + APCI) 476.2 $(M + H)^+$.

2.6.8. 4-(6-bromobenzo[d][1,3]dioxol-5-yl)-3,7,7-trimethyl-1-phenyl-6,7,8,9-tetra-hydro-1H-pyrazolo[3,4-b]quinolin-5(4H)-one. 4h

Yellowish white solid; melting point: 252–255 °C; R_f = 0.65; ^{1}H NMR (400 MHz, DMSO-d_6) (δ, ppm): 7.32–7.44 (m, 5H, ArH), 6.95 (s, 1H, CH), 6.82 (s, 1H, CH), 5.87 (s, 2H, CH_2), 4.99 (s, 1H, CH), 2.35 (s, 2H, CH_2), 2.14 (s, 2H, CH_2), 2.06 (s, 3H, CH_3) 1.02 (s, 6H, CH_3); ^{13}C APT (100 MHz, $CDCl_3$ + DMSO-d_6) (δ, ppm): 195.37, 166.86, 149.95, 147.89, 147.56, 146.47, 140.64, 137.84, 135.60, 135.58, 129.85, 127.56, 127.51, 123.04, 122.98, 113.22, 101.51 71.81, 50.77, 45.34, 42.35, 32.56, 12.72; MS (MM-ES + APCI) 504.3 $(M + H)^+$.

2.6.9. 4-(6-bromobenzo[d][1,3]dioxol-5-yl)-3-methyl-1-phenyl-4,6,7,8-tetrahydro-cyclopenta[b] pyrazolo[4,3-e]pyridin-5(1H)-one. 4i

white solid; melting point: 261–264 °C; R_f = 0.28; ^{1}H NMR (400 MHz, DMSO-d_6) (δ, ppm): 10.22 (s, 1H, NH), 7.40–7.55 (m, 5H, ArH), 7.09 (s, 1H, CH), 6.67 (s, 1H, CH), 6.00 (d, J = 5.2 Hz, 2H, CH_2), 5.21 (s, 1H, CH), 2.66 (dd, J = 4.8 Hz, 6.8 Hz, 2H, CH_2), 2.26 (t, J = 4.8 Hz, 2H, CH_2), 1.84 (s, 3H, CH_3); ^{13}C APT (100 MHz, DMSO-d_6) (δ, ppm): 200.11, 166.80, 166.78, 146.43, 146.38, 137.88, 129.37, 127.07, 123.38, 112.42, 101.75, 33.67, 24.39, 12.26; MS (MM-

Table 1
Optimization of the reaction conditions for the synthesis of **4b**.

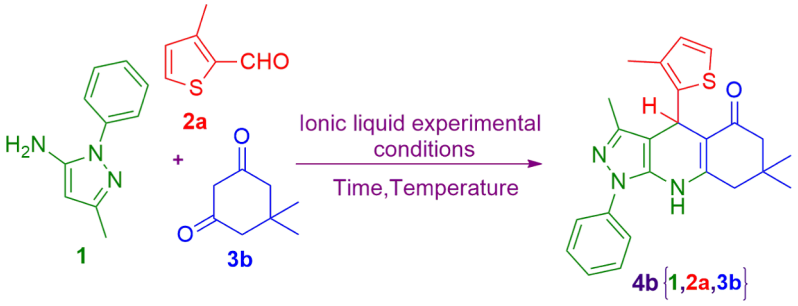

Entry[a]	Ionic liquids	Temp (°C)	Time (min.)	Yield[b] (%)
1	tris(hydroxyethyl)ammoniumacetate [$(HE)_3AAc$]	35	3600	NR
2	bis(2-hydroxyethyl)ammoniumacetate [$(HE)_2AAc$]	35	3600	48
3	2-hydroxyethylammonium lactate [HEALac]	35	3600	55
4	2-hydroxyethylammonium formate [HEAF]	35	3600	62
5	2-hydroxyethylammonium acetate [HEAAc]	35	3600	67
6	2-hydroxyethylammonium acetate [HEAAc]	50	2400	70
7	2-hydroxyethylammonium acetate [HEAAc]	70	180	76
8	2-hydroxyethylammonium acetate [HEAAc]	90	120	84
9	2-hydroxyethylammonium acetate [HEAAc]	95	120	84
10	2-hydroxyethylammonium acetate [HEAAc] (1st run)	90	120	82
11	2-hydroxyethylammonium acetate [HEAAc] (2nd run)	90	180	81
12	2-hydroxyethylammonium acetate [HEAAc] (3rd run)	90	180	77

[a] Reaction conditions: 3-methyl-1-phenyl-1H-pyrazole-5-amine 1 (3 mmol), 5,5-dimethylcyclohexane-1,3-dione 3b (3 mmol), 3-methylthiophene-2-carboxaldehyde 2a (3 mmol), and HEAAc IL (2 mL, ~ 6.3 equiv).
[b] Isolated yield of products.

Table 2
The comparison of the catalytic efficiency of Ionic liquid with other catalysts.

Entry[a]	Catalyst	Solvent	Temp (°C)	Time (min)	Yield[b] (%)	References for reported catalysts
1	L-Proline (10 mol%)	–	MW/110	15	75	[17]
2	PEG-400	–	100–110	240	68	[16]
3	Et_3N (3.6 mmol)	Ethanol	MW/150	15	70	[14]
4	SDS (0.3 gm)	Water	90	420	60	[19]
5	–	Ethanol	Reflux	30	12	–
6	CAN (20 mol%)	Ethanol	Reflux	180	58	–
7	$AlCl_3$ (20 mol%)	Ethanol	Reflux	180	45	–
8	$FeCl_3$ (20 mol%)	Ethanol	Reflux	180	38	–
9	Citric acid (20 mol%)	Ethanol	Reflux	180	46	–
10	–	Glacial acetic acid	RT (35)	180	70	[18]
11	HEAAc (2 mL)	Water	90	180	NR	–
12	HEAAc (2 mL)	Methanol	Reflux	120	66	–
13	HEAAc (2 mL)	Ethanol	Reflux	120	80	–
14	HEAAc (2 mL)	Aqueous ethanol (1:1, v/v)	90	120	60	–
15	HEAAc (2 mL)	Aqueous ethanol (1:1, v/v)	90	120	55	–
16	HEAAc (2 mL)	Neat (IL only)	90	120	84	This work

[a] Reaction conditions: 3-methyl-1-phenyl-1H-pyrazole-5-amine **1** (3 mmol), 5,5-dimethylcyclohexane-1,3-dione **3b** (3 mmol), 3-methylthiophene-2-carboxaldehyde **2a** (3 mmol).
[b] Isolated yield of **4b**.

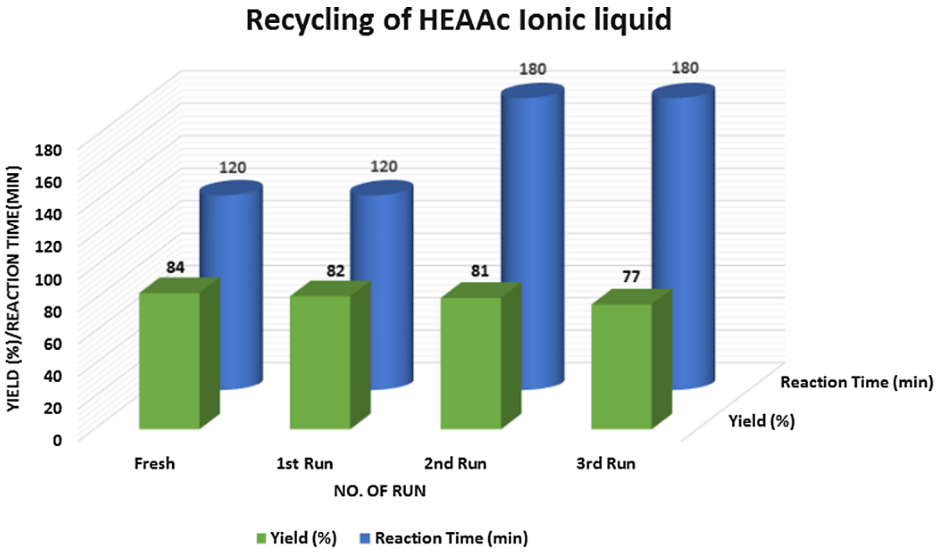

Fig. 3. Recycling of HEAAc Ionic liquid.

ES + APCI) 464.2 $(M + H)^+$.

2.6.10. 4-(2-butyl-5-chloro-1H-imidazol-4-yl)-3-methyl-1-phenyl-6,7,8,9-tetrahydro-1H-pyrazolo [3,4-b]quinolin-5(4H)-one. 4j

Off white solid; melting point: 228–231 °C; $R_f = 0.29$; ^1H NMR (400 MHz, DMSO-d_6) (δ, ppm): 11.81 (s, 1H, NH), 9.57 (s, 1H, NH), 7.39–7.55 (m, 5H, ArH), 5.07 (s, 1H, CH), 2.55–2.68 (m, 2H, CH_2), 2.47 (t, $J = 7.6$ Hz, 2H, CH_2), 2.20–2.245 (m, 2H, CH_2), 1.93(s, 3H, CH_3), 1.82–1.89 (m, 2H, CH_2), 1.55 (quint, $J = 7.6$ Hz, 2H, CH_2), 1.55 (sext, $J = 7.2$ Hz, 2H, CH_2), 0.86 (t, $J = 7.6$ Hz, 2H, CH_2); ^{13}C APT (100 MHz, DMSO-d_6) (δ, ppm): 194.25, 153.80, 145.93, 144.28, 138.16, 136.30, 129.35, 128.68, 126.86, 123.18, 122.13, 106.84, 101.16, 36.91, 29.95, 27.45, 27.37, 26.03, 21.58, 20.96, 13.60, 11.74; MS (MM-ES + APCI) 434.3 $(M + H)^+$.

2.6.11. 4-(2-butyl-5-chloro-1H-imidazol-4-yl)-3,7,7-trimethyl-1-phenyl-6,7,8,9-tetra-hydro-1H-pyrazolo[3,4-b]quinolin-5(4H)-one. 4k

White solid; melting point: 183–186 °C; $R_f = 0.34$; ^1H NMR (400 MHz, DMSO-d_6) (δ, ppm): 11.75 (s, 1H, NH), 9.40 (s, 1H, NH), 7.33–7.49 (m, 5H, ArH), 5.06 (s, 1H, CH), 2.46–2.51 (m, 2H, CH_2), 2.03–2.16 (m, 2H, CH_2), 1.92 (s, 3H, CH_3), 1.56 (quint, $J = 7.6$ Hz, 2H, CH_2), 1.27 (t, $J = 8$ Hz, 2H, CH_2), 1.23 (s, 2H, CH_2), 1.01 (d, $J = 8$ Hz, 6H, CH_3), 0.87 (t, $J = 3.6$ Hz, 2H, CH_2); ^{13}C APT (100 MHz, DMSO-d_6) (δ, ppm): 193.97, 151.51, 146.07, 144.25, 138.20, 136.49, 129.04, 128.64, 126.50, 122.98, 122.32, 106.03, 101.04, 50.47, 40.69, 31.70, 30.03, 28.79, 27.61, 27.02, 26.03, 21.61, 13.52, 11.61; MS (MM-ES + APCI) 462.3 $(M + H)^+$.

2.6.12. 4-(2-butyl-5-chloro-1H-imidazol-4-yl)-3-methyl-1-phenyl-4,6,7,8-tetrahydro-cyclopenta[b] pyrazolo[4,3-e]pyridin-5(1H)-one. 4l

Off white solid; melting point: 179–182 °C; $R_f = 0.20$; ^1H NMR (400 MHz, DMSO-d_6) (δ, ppm): 11.73 (s, 1H, NH), 10.23 (s, 1H, NH), 7.40–7.58 (m, 5H, ArH), 4.88 (s, 1H, CH), 2.64 (s, 2H, CH_2), 2.45–2.49 (t, 2H, CH_2), 2.29 (d, $J = 2.0$ Hz, 2H, CH_2), 1.86 (s, 3H, CH_3), 1.55 (quint, $J = 7.6$ Hz, 2H, CH_2), 1.26 (sext, $J = 7.2$ Hz, 2H, CH_2), 0.86 (t, $J = 7.2$ Hz, 3H, CH_3); ^{13}C APT (100 MHz, DMSO-d_6) (δ, ppm): 200.66, 167.50, 146.95, 145.73, 138.44, 138.37, 129.92, 127.55, 127.02, 123.72, 123.16, 112.29, 101.58, 34.17, 30.40, 28.00, 25.73, 24.88, 22.09, 14.10, 12.25; MS (MM-ES + APCI) 420.3 $(M + H)^+$.

2.6.13. 3-methyl-1-phenyl-4-(thiophen-2-yl)-6,7,8,9-tetrahydro-1H-pyrazolo[3,4-b]quinolin-5(4H)-one. 4m

Off white solid; melting point: 212–215 °C; $R_f = 0.31$; ^1H NMR (400 MHz, $CDCl_3$) (δ, ppm): 7.32–7.46 (m, 5H, ArH), 7.15 (s, 1H,

Thiophene-CH), 7.08 (s, 1H, Thiophene-CH), 6.87 (s, 1H, Thiophene-CH), 5.53 (s, 1H, CH), 2.46–2.52 (m, 2H, CH_2), 2.27–2.40 (m, 2H, CH_2), 2.16 (s, 3H, CH_3), 1.94–1.99 40 (m, 2H, CH_2); ^{13}C APT (100 MHz, $CDCl_3$) (δ, ppm): 195.73, 151.38, 151.03 147.51, 137.96, 135.66, 129.83, 127.44, 126.43, 123.67, 123.54, 123.01, 112.79, 104.03, 37.08, 30.57, 28.66, 21.10, 12.18; MS (MM-ES + APCI) 360.2 $(M + H)^+$.

2.6.14. 3,7,7-trimethyl-1-phenyl-4-(thiophen-2-yl)-6,7,8,9-tetrahydro-1H-pyrazolo[3,4-b]quinolin-5 (4H)-one. 4n

Off white solid; melting point: 226–229 °C; R_f = 0.51; ^{1}H NMR (400 MHz, $CDCl_3$) (δ, ppm): 7.35–7.48 (m, 5H, ArH), 7.06 (d, J = 5.2 Hz, 1H, Thiophene-CH), 6.84 (d, J = 3.6 Hz, 1H, Thiophene-CH), 6.69 (s, 1H, Thiophene-CH), 5.52 (s, 1H, CH), 2.35 (s, 2H, CH_2), 2.24 (s, 2H, CH_2), 2.16 (s, 3H, CH_3), 1.05 (d, J = 7.2 Hz, 6H, CH_3); ^{13}C APT (100 MHz, $CDCl_3$) (δ, ppm): 195.42, 151.11, 148.87, 147.56, 135.64, 129.95, 127.53, 126.40, 123.66, 123.53, 122.90, 111.74, 104.10, 50.80, 42.39, 32.57, 30.61, 29.13, 27.35, 12.16; MS (MM-ES + APCI) 388.2 $(M + H)^+$.

2.6.15. 3-methyl-1-phenyl-4-(thiophen-2-yl)-4,6,7,8-tetrahydrocyclopenta[b]pyrazolo-[4,3-e] pyridin-5(1H)-one. 4o

White solid; melting point: 233–236 °C; R_f = 0.22; ^{1}H NMR (400 MHz, DMSO-d_6) (δ, ppm): 10.01 (s, 1H, NH), 7.21–7.36 (m, 5H, ArH), 6.99 (d, J = 5.2 Hz, 1H, Thiophene-CH), 6.75 (d, J = 3.2 Hz, 1H, Thiophene-CH), 6.68 (d, J = 3.6 Hz, 1H, Thiophene-CH), 5.03 (s, 1H, CH), 2.36 (t, J = 1.6 Hz 2H, CH_2), 2.16 (m, 2H, CH_2), 2.16 (t, J = 3.6 Hz 2H, CH_2), 1.81 (s, 3H, CH_3); ^{13}C APT (100 MHz, DMSO-d_6) (δ, ppm): 200.31, 165.94, 150.36, 146.71, 137.88, 137.50, 129.15, 128.82, 126.79, 126.11, 123.51, 123.10, 114.89, 103.13, 33.71, 29.90, 24.17, 12.06; MS (MM-ES + APCI) 346.2 $(M + H)^+$.

2.7. Biological evaluation

2.7.1. In vitro antimicrobial activity

This study was screened against 24 h old bacterial cultures which include two Gram-positive, two Gram-negative bacteria and three fungi via the use of disc diffusion method according to the National Committee for Clinical Laboratory Standards (NCCLS) [40]. Muller-Hinton Broth was used as a nutrient medium to grow and dilute the drug suspension for the test bacteria and sabouraud dextrose broth was used for nutrition of the fungi. All the synthesized compounds were screened at 1000 ppm in DMSO solution. The strains which were used for this study were attained from MTCC, Institute of Microbial Technology, Chandigarh. The synthesized compounds **4(a-o)** were screened for their antibacterial activity against Gram-negative bacteria like *E. Coli* (MTCC 443), *P. Aeruginosa* (MTCC 96), and against Gram-positive bacteria such as *S. aureus*(MTCC 96) and *S. Pyogenus*(MTCC 442) and their antifungal screening was performed against *C. Albicans* (MTCC 227), *A. Niger* (MTCC 282) and *A. Clavatus* (MTCC 1323). In this study, the standard drugs used for the comparison of antibacterial activity were ampicillin, chloramphenicol, ciprofloxacin, norfloxacin whereas nystatin and griseofulvin were used as standard drugs for the antifungal activity.

2.7.2. In vitro antituberculosis activity

The encouraging results from the antibacterial studies impelled us for preliminary screening of all newly synthesized compounds against *Mycobacterium tuberculosis*. In this screening, 1000, 500, and 250 μg/ml concentrations of the compounds were taken. The active compounds found in this screening were further tested in a secondary screening against *M. tuberculosis* H37Rv in L. J. Medium (conventional method). The compounds found active in primary screening were similarly diluted to obtain 200, 100, 50, 25, 12.5, 6.250, and 3.50 μg/ml concentrations. The antitubercular activity data were compared with rifampicin at a 40 μg/ml concentration. All the values of MIC (μg mL^{-1}) are provided for 99% inhibition of *M. tuberculosis* growth. As shown in Table 5.

2.7.3. In vitro antiproliferative activity

The anti-proliferative activity of the reported compounds was studied using our implementation of the NCI protocol [41] against human solid tumor cell lines (A549, HBL-100, HeLa, SW1573, T-47D, WiDr) and the human fibroblast cell line BJ-hTert kindly provided by Dr. G. J. Peters (The Netherlands) and Dr. Raimundo Freire (Canary Islands). The results are expressed as GI_{50} (dose that produces 50% growth inhibition) and were determined for an exposure time of 48 h. Cell line suspensions were counted with Moxi Z and diluted to reach the appropriate cell densities (A549, HBL-100, HeLa and SW1573 2500 cells/well; T-47D and WiDr 5000 cells/well; BJ-hTert 4000 cells/well) for inoculation onto 96-well plates. After 24 h, pure compounds were added. Each agent was initially dissolved in DMSO at 400 times the desired final maximum test concentration (100 μM). Control cell samples were exposed to an equivalent concentration of DMSO (0.25% v/v, negative control). Compounds were tested at serial dilutions (0.01–100 μM).

3. Results and discussion

3.1. Chemistry

In the present protocol, we selected one-pot fusion of 3-methyl-1-phenyl-1H-pyrazole-5-amine **1** (3 mmol), 3-methylthiophene-2-carboxaldehyde **2a** (3 mmol) and 5, 5-Dimethyl-1, 3-dione **3b** (3 mmol) in the

Table 3
Synthesis of functionalized pyrazolodihydropyridine derivatives **4(a-o)**[a].

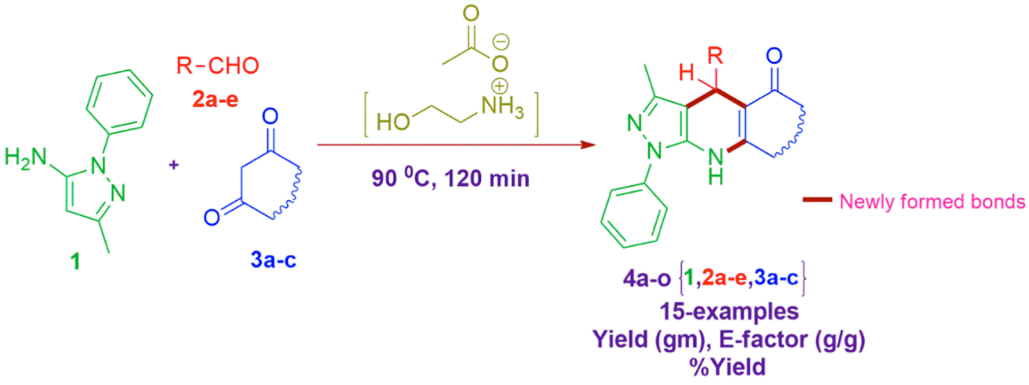

(continued on next page)

Table 3 (*continued*)

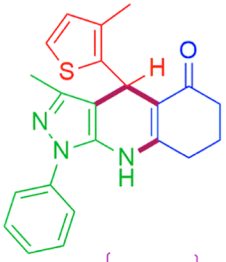

4a {1,2a,3a}
0.89 gm, 0.39 g/g
79%

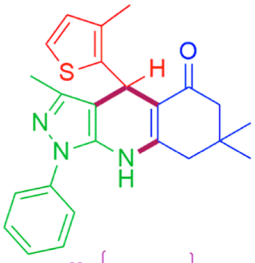

4b {1,2a,3b}
1.01 gm, 0.30 g/g
84%

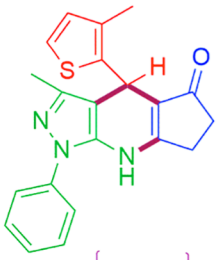

4c {1,2a,3c}
0.77 gm, 0.54 g/g
71%

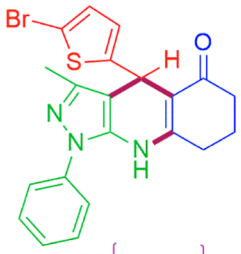

4d {1,2b,3a}
1.14 gm, 0.25 g/g
87%

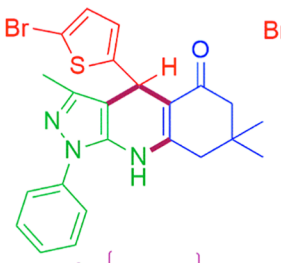

4e {1,2b,3b}
1.25 gm, 0.21 g/g
89%

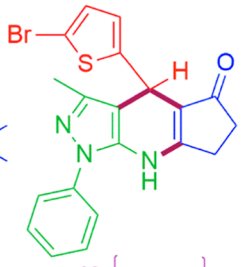

4f {1,2b,3c}
0.79 gm, 0.75 g/g
62%

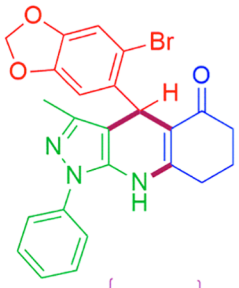

4g {1,2c,3a}
1.06 gm, 0.45 g/g
74%

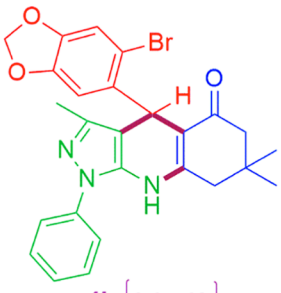

4h {1,2c,3b}
1.17 gm, 0.38 g/g
77%

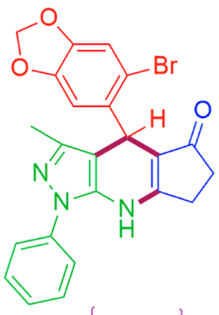

4i {1,2c,3c}
0.84 gm, 0.78 g/g
60%

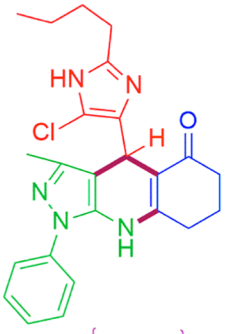

4j {1,2d,3a}
1.02 gm, 0.38 g/g
78%

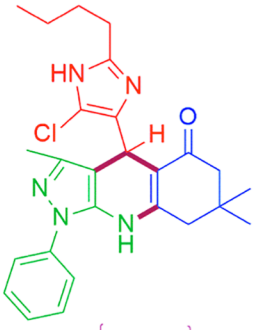

4k {1,2d,3b}
1.14 gm, 0.31 g/g
82%

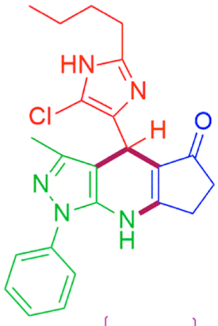

4l {1,2d,3c}
0.81 gm, 0.69 g/g
64%

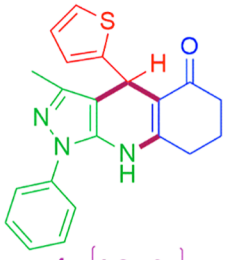

4m{1,2e,3a}
0.85 gm, 0.40 g/g
78%

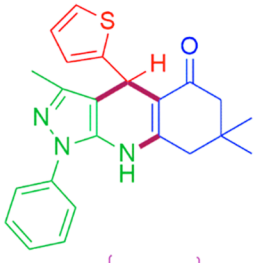

4n {1,2e,3b}
0.95 gm, 0.34 g/g
82%

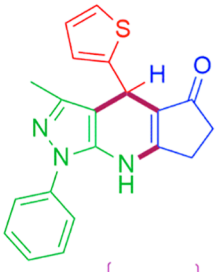

4o {1,2e,3c}
0.73 gm, 0.57 g/g
70%

Table 4
Gram-scale synthesis of **4b**.

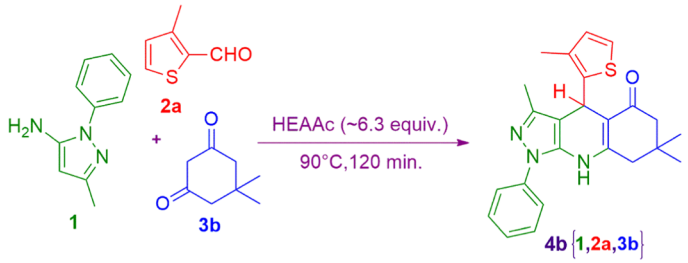

Entry[a]	Batch amount (mmol)	Purification Technique	Yield[b] (%)	Yield[b] (gm)
1	3.0	Column Chromatography	84	1.01
2	5.0	Column Chromatography	82	1.67
3	10.0	Column Chromatography	80	3.23

[a] Reaction conditions: 3-methyl-1-phenyl-1H-pyrazole-5-amine **1** (1 equiv), 5,5-dimethylcyclohexane-1,3-dione **3b** (1 equiv.), 3-methylthiophene-2-carboxaldehyde **2a** (1 equiv).
[b] Isolated yield of **4b**.

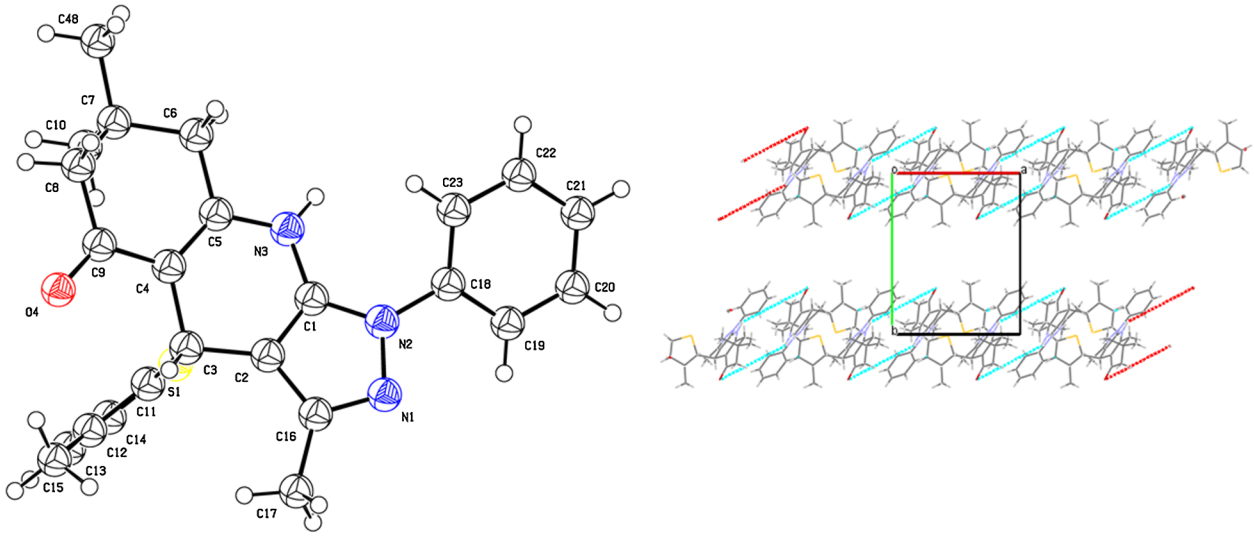

Fig. 4. X-ray structure of **4b (CCDC 1837695)**, ellipsoid are drawn at the 50% probability level and crystal packing view along the c-axis showing dimer held together by N-H—O hydrogen bonds.

presence of different hydroxyl alkyl ammonium ionic liquids as a model reaction. As shown in Fig. 2.

During the optimization of reaction conditions, we made attempt to scale down the amount of ionic liquid 0.5 and 1.0 mL which equal to ~4.7 mmol and 9.5 mmol respectively (density = 1.149039 g cm^{-3}; M_w = 121.14 g mol^{-1}) [39]. Unfortunately, we observed solidification of the reaction mass and no complete consumption of starting materials. This problem was overcome by loading a minimum 1.5 mL or more amount of ionic liquid. Here we carried out the synthesis of **4b** using different hydroxyl alkyl ammonium ionic liquids under different reaction conditions as shown in Table 1 (1–12 entries). Our first attempt was to synthesize **4b** at ambient temperature condition using different hydroxyl alkyl ammonium ionic liquids. But at ambient temperature condition, we observed that $(HE)_3AAc$ IL shows no reaction transformation, and satisfactory reaction transformation observed in case of $(HE)_2AAc$, HEALac, HEAF, and HEAAc isolated yields are 48%, 55%, 62%, and 67% respectively. Among all ILs best result obtained with HEAAc (2 mL, ~6.3 equiv). So we selected HEAAc IL to synthesize desired products. In order to reduce the reaction time and achieving the complete conversion of starting materials into desired products, we go further for the screening of temperature and different solvents. Here we carried out the reaction using different hydroxyl alkyl ammonium ionic liquids at different temperatures (Table 1) and also compared the catalytic efficiency of HEAAc IL with some reported and non-reported catalysts (Table 2, entries 1–16) as well. After analyzing all the results collected from optimization of the reaction parameters, the excellent yield is obtained when the reaction is carried out using HEAAc (2 mL, ~6.3 equiv.) at 90 °C under neat condition. We did not find any significant increment in the yield of the desired product for the temperature range beyond 90 °C. Therefore, we selected it as the optimal reaction temperature for all these reactions.

3.1.1. Procedure for catalyst recycling

After completion of the reaction, the mixture was poured into ice cold water and filtered off. The filtrate containing IL was then charged in Rota evaporator and recovered by removing excess water under reduced pressure at 60–70 °C and was reused up to three more runs for subsequent reactions (without considering fresh run). Up to the second run (without considering fresh run), there is no significant change in the yield of the desired product (See Fig. 3).

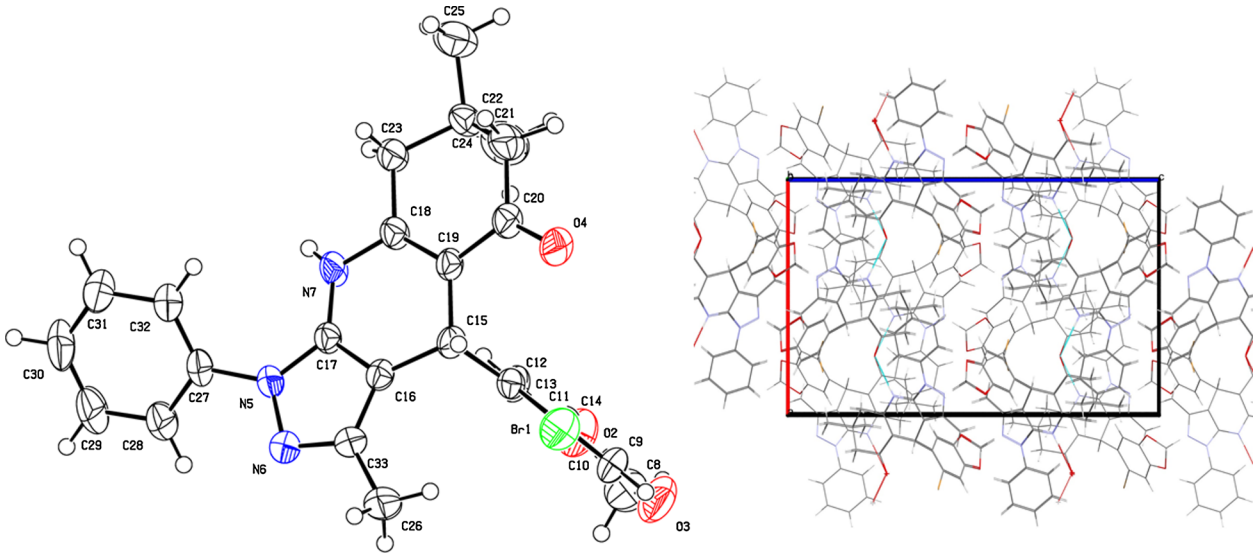

Fig. 5. X-ray structure of **4h (CCDC 1838422),** ellipsoid are drawn at the 50% probability level and Crystal packing view along the b-axis showing dimer held together by N-H—O hydrogen bonds.

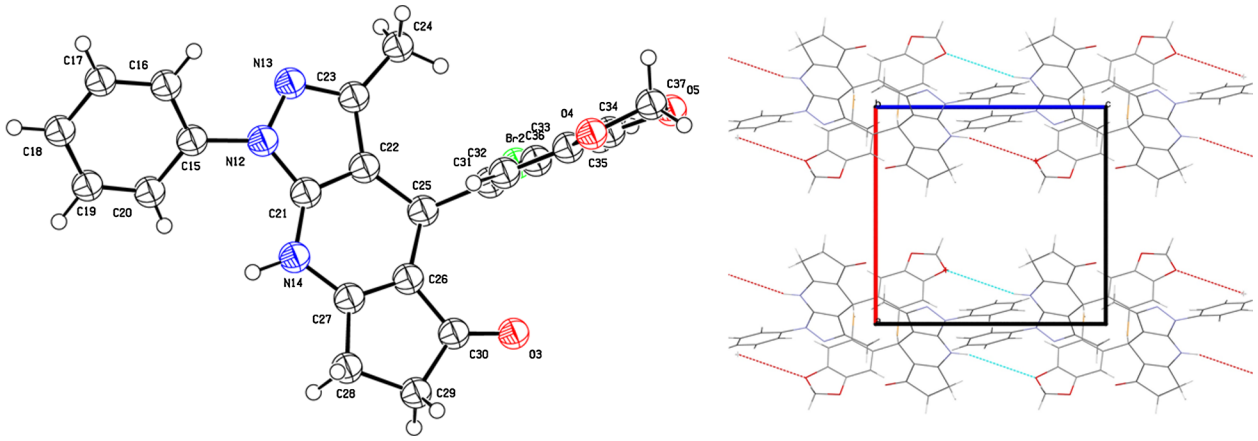

Fig. 6. X-ray structure of **4i (CCDC 1838423)**, ellipsoid are drawn at the 50% probability level and crystal packing view along the b-axis showing dimer held together by N-H—O hydrogen bonds.

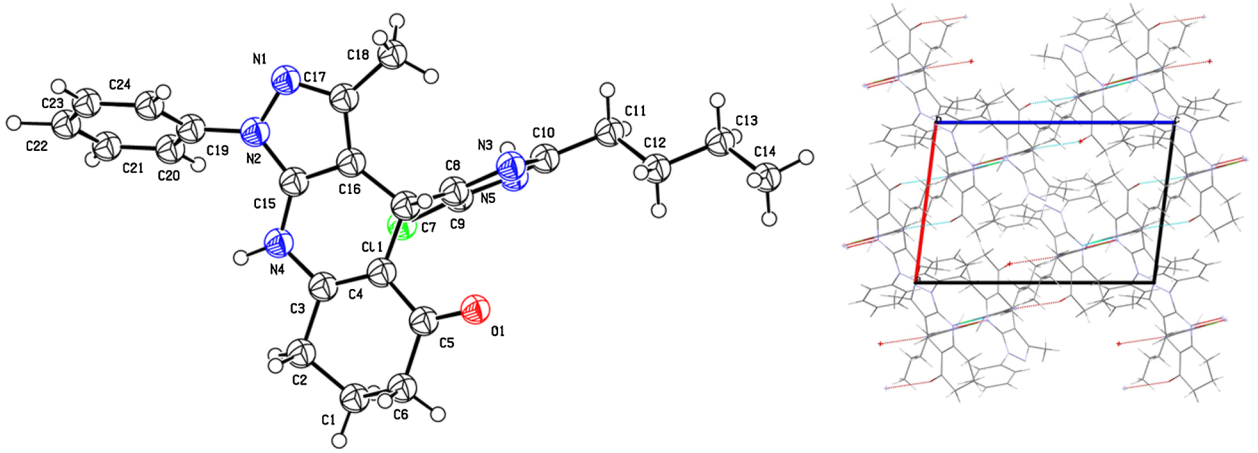

Fig. 7. X-ray structure of **4j (CCDC 1837016)**, ellipsoid are drawn at the 50% probability level and crystal packing arrangement view along the b-axis showing dimer held together by N-H—O hydrogen bonds.

The synthesis of pyrazolodihydropyridine derivatives was carried out under the optimized reaction conditions of HEAAc with 3-methyl-1-phenyl-1H-pyrazole-5-amine **1**, 1,3-diones **2(a-c)**, and different aldehydes **3 (a-e)**. To our delight, all the reactions proceed smoothly under optimized reaction conditions and the isolated yields of desired products were in the range of 60–89% and as shown in Table 3.

Table 5
Synthesis of the compound **4b** using different ILs or molten salts under optimized reaction conditions.

Entry[a]	ILs or molten salts	Reaction time (min.)	% Yield[b]
1	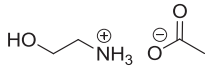	120	84
2	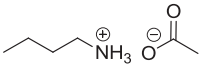	120	38
3	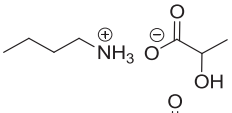	120	30
4	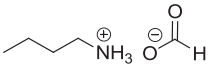	120	25
5	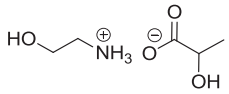	120	79
6	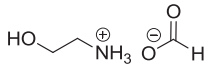	120	75

[a] Reaction conditions: 3-methyl-1-phenyl-1H-pyrazole-5-amine **1** (3 mmol), 5,5-dimethylcyclohexane-1,3-dione **3b** (3 mmol), 3-methylthiophene-2-carboxaldehyde **2a** (3 mmol).
[b] Isolated yield of **4b**.

As an efficient and economic protocol, the scale-up and operational simplicity are also important parameters thus the different scale reactions of 3-methyl-1-phenyl-1H-pyrazole-5-amine **1** (1 equiv.), 5,5-dimethylcyclohexane-1,3-dione **3b** (1 equiv), and 3-methylthiophene-2-carboxaldehyde **2a** (1 equiv) under optimized reaction conditions were carried out. The scale-up outcomes are shown in Table 4.

In the preliminary investigation desired product formation was confirmed by thin layer chromatographic Technique using 50% ethyl acetate in petroleum ether (60–80 °C) as a mobile phase. The structure of all desired compounds was unambiguously confirmed by ^{1}H NMR, ^{13}C- NMR, and MS spectroscopic techniques. For further verification of the desired products **4b**, **4h**, **4i**, and **4j** were selected as representative compounds and were confirmed by single-crystal X-ray diffraction analysis, as shown in Figs. 4–7.

In order to justify the role of hydroxyl group present in the structure of hydroxyl alkyl ammonium ionic liquid during the reaction transformation herein, we carried out similar experiments which were reported by Moones Honarmand et al. [42]. Here we synthesized some −OH functional group free ionic liquids/molten salts using *n*-butyl amine with acids (formic acid, acetic acid, and lactic acid) and used them as catalysts for the synthesis of compound **4b** under optimized reaction conditions. Noteworthy, we made a comparison between the results obtained (in terms of yield of desired product) from −OH functional group free ILs with −OH functional group containing ILs. From this comparison, we confirmed that the presence of −OH functional group in the structure of hydroxyl alkyl ammonium ILs makes a significant contribution during reaction transformation. We also synthesized compound **4b** by replacing the counter anions (formate, acetate, and lactate) in order to check the catalytic efficiency but we did not find any remarkable change in the yield of compound **4b** under these catalytic conditions (See the Table 5).

Thus on the bases of these facts, we proposed a possible mechanistic path for the synthesis of functionalized pyrazolodihydropyridine derivatives using HEAAc IL. In the structure of hydroxyl ethyl ammonium acetate ionic liquid, the presence of quaternary ammonium group acts as proton donor while ephemerally generated hydroxyl alkyl amine during reaction transformation can act as a base. The presence of quaternary ammonium part in the structure of ionic liquid can activate the aldehyde by protonating it. While ephemerally generated 2-aminoethanol can play the role as a base to deprotonate C—H acid (1, 3-diones **3a-c**) to generate active enolates which can make a subsequent nucleophilic attack on protonated aldehyde and produce alcoholic derivatives. The presence of acidic protons from ammonium ions of 2-hydroxyethylammonium acetate can facilitate the elimination of first water molecule and afford α, β-unsaturated dicarbonyl derivatives, which can further undergo nucleophilic attack by 3-methyl-1-phenyl-1H-pyrazole-5-amine **1** to beget tautomerized imine derivatives. The cyclization step can be accomplished by nucleophilic attack of the primary amine group on hydrogen bonded carbonyl group. In final step protonation on alcoholic group followed by subsequent deprotonation by the ionic liquid can afford desire products and regenerate the ionic liquid along with the elimination of second water molecule. (See Scheme 2).

3.2. Biological results

3.2.1. In vitro antibacterial screening

After analyzing the antibacterial screening data (see the Table 6), it has been concluded that majority of the synthesized compounds showed potency against *E. coli*, *P. aeruginosa*, *S. aeruginosa,* and *S. pneumoniae* compared to the standard drug ampicillin. In comparison to the standard drug ampicillin (MIC 100 μg mL^{-1}) against Gram-negative bacteria, against *E. coli* compound **4c** shows better potency (MIC 50 μg mL^{-1}) whereas **4b, 4e, 4g, 4j,** and **4n** show equipotency; against *P. aeruginosa* compounds **4d** and **4i** were found potent whereas compounds **4b, 4e, 4m,** and **4n** show same potency to that of ampicillin. While in the case of inhibition of Gram-positive bacteria against *S. aeruginosa* compounds **4c, 4g, 4i, 4l, 4m,** and **4o** show excellent potency whereas **4b, 4d, 4e, 4h, 4k, 4n** facilitate equipotency to that of ampicillin. Among all these compounds **4i** show outstanding activity (MIC 12.5 μg mL^{-1}) against *S. aeruginosa* which is far better than ampicillin, chloramphenicol, and ciprofloxacin.

3.2.2. In vitro antifungal screening

The data collection from *In vitro* antifungal screening it has been observed that, against *C. albicans*, compounds **4e, 4g, 4i, 4l, 4m, and 4o** show better activity than standard drug griseofulvin (MIC 500 μg mL^{-1}), among these compounds **4m** show far better potency than that of griseofulvin and show equipotency to nystatin (MIC 100 μg mL^{-1}). All the compounds showed poor inhibition against *A.niger* and *A. clavatus.* As shown in Table 6.

3.2.3. In vitro antitubercular screening

From the results of the antitubercular screening of targeted synthesized compounds, we found compound **4o** (MIC 25 μg mL^{-1}) far potent than rifampicin (MIC 40 μg mL^{-1}) as shown in Table 7. All other compounds show poor inhibition of *M. tuberculosis*.

3.2.4. In vitro antiproliferative screening

Table 8 shows the results of antiproliferative assays against human solid tumor cells of compounds **4(a-o)**. The standard anticancer drug cisplatin (CDDP) was used as reference drug. Overall, the results expressed as GI_{50} after 48 h of exposure show that compounds are modest inhibitors of cancer cell growth. The most active compounds of the series are **4f** and **4i**, which show GI_{50} values in the range 16–33 μM. In order to check for selectivity towards healthy cells, those compounds active against all cell lines (**4a-b**, **4d**, **4f**, **4i**) were tested in the human fibroblast cell line BJ-hTert. The GI_{50} values obtained for all compounds were $>$ 100 μM, indicating no antiproliferative activity in normal cells and a good selectivity. Noteworthy, CDDP shows a GI_{50} of 14 $\pm$ 2.4 μM in BJ-hTert cells.

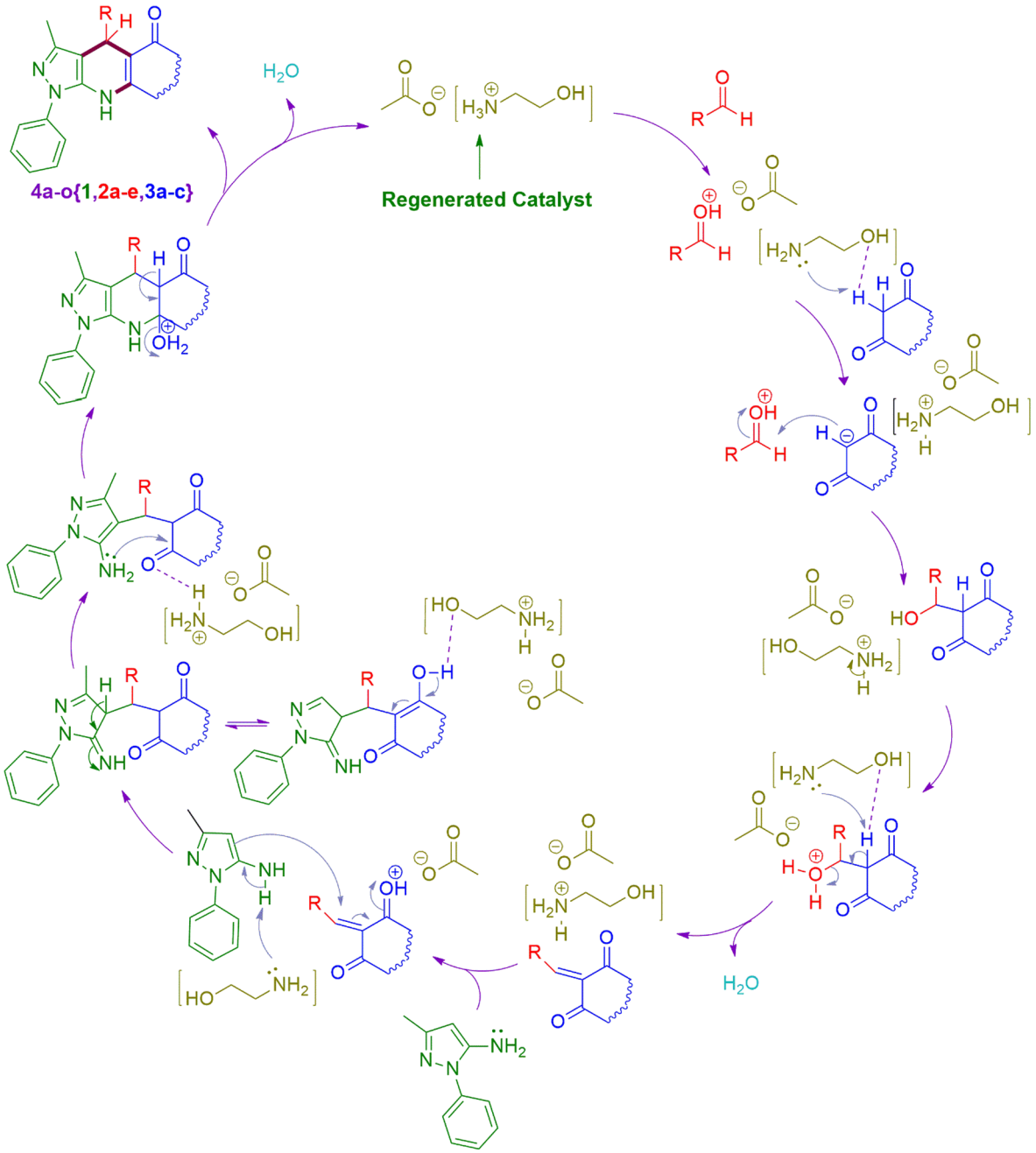

Scheme 2. The possible mechanistic pathway to approach functionalized pyrazolodihydropyridine derivatives **4a-o** using HEAAc IL.

3.2.5. Structural-activity relationship (SAR)

A detailed study on the obtained results from *in-vitro* biological screening of all synthesized compounds, we found that the attachment of the different heterocyclic aldehydes at the C-4 position and fusion of the six-membered or five-membered ring with basic moiety are responsible for showing the biological activities. The substitution at C-4 position of six-membered fused pyrazolodihydropyridine core by 5-bromothiophene increase the antibacterial, antifungal, and antitubercular activities against *P. aeruginosa*, *C. albicans,* and *M. Tuberculosis* pathogenic strains respectively. In a similar manner substitution by 6-bromopiperonyl and thiophene increase the antifungal activity against *C. albicans* pathogenic strains. Noteworthy, substitution at the C-4 position of five-membered fused pyrazolodihydropyridine derivatives by 3-methyl thiophene substituent increase the antibacterial activity against *E. coli* and *S. aeruginosa* whereas, substitution by 5-bromothiophene showed potency against cervix solid tumor cell line. In similar trend attachment of 6-bromopiperonyl increase the antibacterial activity against *P. aeruginosa* and *S. aeruginosa*, additionally, the same group attachment also showed potent inhibition against Cervix, breast, and colon solid tumor cell lines. The presence of a thiophene group at the C-4 position is responsible for increasing antifungal activity and antitubercular activity against *C. albicans* and *M. Tuberculosis* respectively (see Fig. 8).

Table 6
In vitro antimicrobial activity (MIC, μg mL^{-1}) of the synthesized compounds **4(a-o)**.

Entry	Gram-negative bacteria		Gram-positive bacteria		Fungi		
	E.C. MTCC 443	*P.A.* MTCC 1688	*S.A.* MTCC 96	*S.P.* MTCC 442	*C.A.* MTCC 227	*A.N.* MTCC 282	*A.C.* MTCC 1323
4a	250	500	500	500	500	> 1000	> 1000
4b	100	100	250	100	1000	1000	1000
4c	**50**	250	**50**	500	500	> 1000	> 1000
4d	125	**62.5**	250	100	500	500	500
4e	100	100	250	500	**250**	1000	1000
4f	250	250	500	500	500	> 1000	> 1000
4g	100	250	200	250	**250**	500	1000
4h	500	500	250	500	500	1000	1000
4i	250	**62.5**	**12.5**	250	**250**	> 1000	> 1000
4j	100	250	500	500	1000	1000	1000
4k	250	500	250	500	500	500	500
4l	500	250	125	100	**250**	1000	1000
4m	500	100	100	250	**100**	1000	> 1000
4n	100	100	250	250	1000	1000	1000
4o	250	125	100	250	**250**	1000	> 1000
Ampicillin	**100**	**100**	**250**	**100**	–	–	–
Chloramphenicol	**50**	**50**	**50**	**50**	–	–	–
Ciprofloxacin	**25**	**25**	**50**	**50**	–	–	–
Norfloxacin	**10**	**10**	**10**	**10**	–	–	–
Nystatin	–	–	–	–	100	100	100
Griseofulvin	–	–	–	–	500	100	100

Bold values show the potent compound; *E.C., Escherichia coli; P.A., Pseudomonas aeruginosa; S.A., Staphylococcus aeruginosa; S.P., Streptococcus pneumoniae; C.A., Candida albicans; A.N., Aspergillus niger; A.C., Aspergillus clavatus;* MTCC., microbial-type culture collection; '—'indicates not tested.

Table 7
In vitro antitubercular activity (MIC, μg mL^{-1}) of the synthesized compounds **4(a-o)**.

Entry	MIC μg/ml	Entry	MIC μg/ml
4a	125	**4i**	250
4b	500	**4j**	500
4c	250	**4k**	100
4d	250	**4l**	500
4e	**62.5**	**4m**	250
4f	250	**4n**	250
4g	125	**4o**	**25**
4h	250		

4. Conclusion

The present study promisingly facilitates the synthesis of functionalized pyrazolodihydropyridine core using hydroxyl alkyl ammonium ionic liquids. These ionic liquids can be easily synthesized in the laboratory with minimum effort and chemicals used to synthesize the ionic liquid are commercially available at low cost. The dual catalytic influence and reusability make it task-specific ionic liquid. The present methodology is environmentally sound, high atom economic, low environment factor, applicable for gram-scale synthesis, and produces water as a byproduct. All the synthesized compounds were tested for various biological activities with the hope for finding new agents which possess excellent antimicrobial, antitubercular and antiproliferative activities. Compound **4c** shows better potency than the standard drug ampicillin against Gram-negative bacteria, against *E. coli* whereas **4b, 4e, 4g, 4j,** and **4n** show equipotency; the compounds **4d** and **4i** exhibited better potency against *P. aeruginosa* than that of ampicillin. Among all compounds, **4i** show outstanding activity against *S. aeruginosa* which is far better than ampicillin, Chloramphenicol, and Ciprofloxacin. The compound **4m** show far better potency against *C. albicans*, than that of griseofulvin and show equipotency to nystatin whereas, in case of antitubercular screening, the compound **4o** was

Table 8
Antiproliferative activity (GI_{50}) of compounds **4(a-o)** against human solid tumor cell lines[a].

Compound	A549 (lung)	HBL-100 (breast)	HeLa (cervix)	SW1573 (lung)	T-47D (breast)	WiDr (colon)
4a	31 ± 1.7	53 ± 2.2	31 ± 1.7	57 ± 13	31 ± 3.0	34 ± 4.8
4b	31 ± 3.9	50 ± 9.5	32 ± 3.1	57 ± 4.2	52 ± 2.8	47 ± 14
4c	84 ± 5.3	> 100	> 100	> 100	> 100	> 100
4d	35 ± 6.9	67 ± 15	34 ± 4.8	91 ± 9.4	34 ± 4.4	39 ± 3.8
4e	46 ± 4.6	95 ± 8.2	33 ± 4.9	98 ± 3.6	> 100	> 100
4f	23 ± 3.0	27 ± 5.5	18 ± 4.4	28 ± 5.4	**20 ± 5.6**	**21 ± 5.6**
4g	> 100	> 100	> 100	> 100	> 100	> 100
4h	71 ± 2.1	> 100	38 ± 2.2	> 100	> 100	> 100
4i	24 ± 2.5	29 ± 5.9	16 ± 2.2	33 ± 7.5	26 ± 3.8	**28 ± 5.1**
4j	> 100	> 100	> 100	> 100	> 100	> 100
4k	> 100	> 100	> 100	> 100	> 100	> 100
4l	> 100	> 100	> 100	> 100	> 100	> 100
4m	> 100	> 100	> 100	> 100	> 100	> 100
4n	83 ± 12	> 100	74 ± 9.0	> 100	> 100	> 100
4o	> 100	> 100	> 100	> 100	> 100	> 100
CDDP	4.9 ± 0.2	1.9 ± 0.2	1.8 ± 0.5	2.7 ± 0.4	17 ± 3.3	23 ± 4.3

[a] Values are mean of two to four independent experiments ± standard deviation.

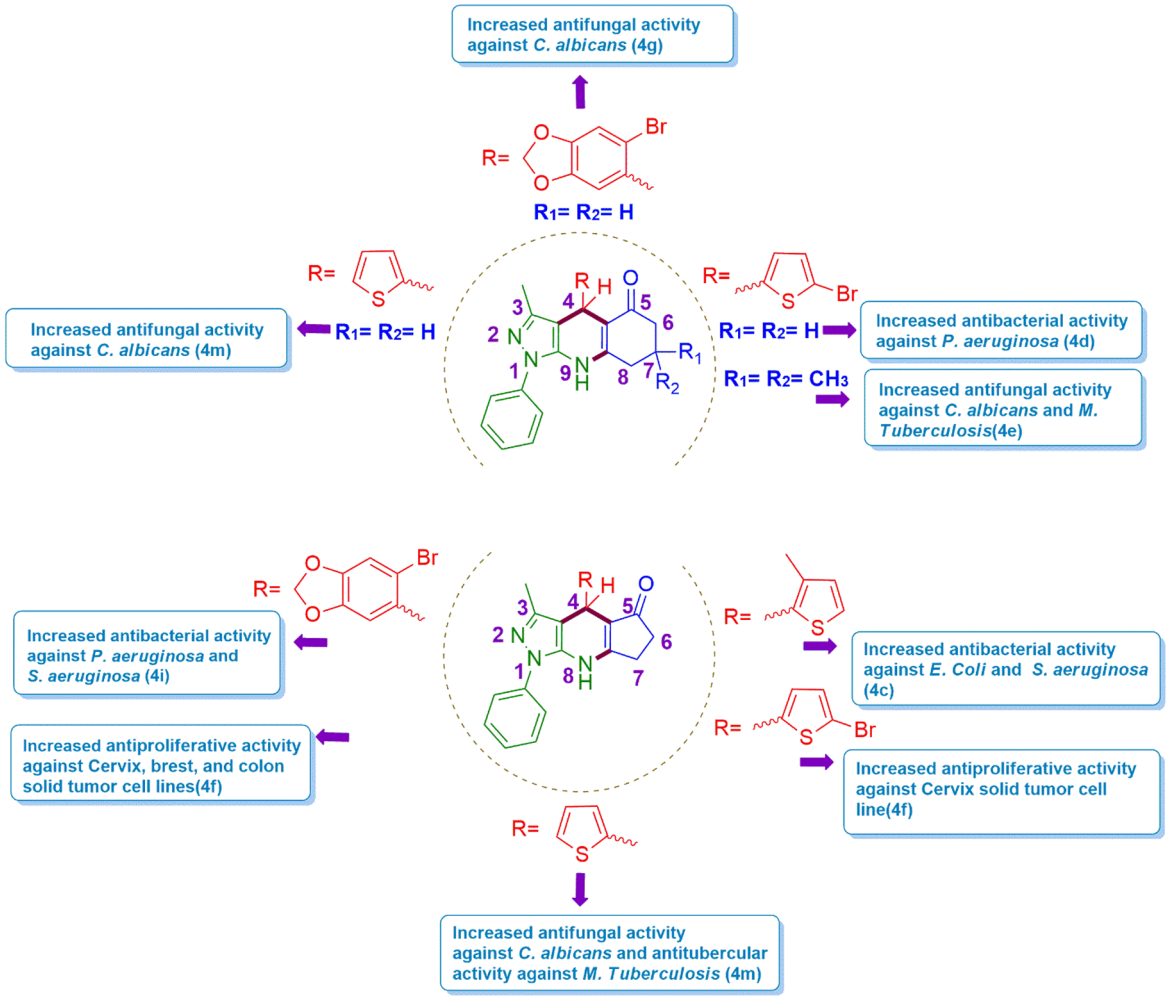

Fig. 8. Structure activity relationship for the in-vitro antimicrobial, antitubercular, and antiproliferative activities.

found more potent than rifampicin. The compounds **4f** and **4i** were found most active in antiproliferative screening.

Acknowledgments

This research was supported by the Department of Chemistry, Sardar Patel University. All the authors are grateful to DST-SERB, New Delhi, India, for providing research grant (File no. EEQ/2016/000376, dated 07/02/2017) and UGC-CPEPA, New Delhi, India, phase-II for the assistance in general and for the NMR facility in particular, sponsored under award letter no. F. No. 1-14/2002-2016(NS/PE) dated 28th April 2016. The Authors are also thankful to Analytical scientist Mr. Milan Ramavat, Aether Industries Ltd. Surat for analytical testing.

Appendix A. Supplementary material

All the spectroscopic and analytical data as well as the copy of ^{1}H-NMR and ^{13}C-APT spectra of all new compounds (PDF) and X-ray crystallographic data of compounds **4b (CCDC 1837695), 4h (CCDC 1838422), 4i (CCDC 1838423), 4j (CCDC 1837016).** Supplementary data to this article can be found online at https://doi.org/10.1016/j.bioorg.2019.01.029.

References

[1] A.M. Akondi, S. Mekala, M.L. Kantam, R. Trivedi, L. Raju, Chowhane, A. Das, New J. Chem. 41 (2017) 873–878.
[2] N.P. Kumar, P. Sharma, T.S. Reddy, S. Nekkanti, N. Shankaraiah, G. Lalita, S. Sujanakumari, S.K. Bhargava, V.G.M. Naidu, A. Kamal, Eur. J. Med. Chem. 127 (2017) 305–317.
[3] N. Jeedimalla, M. Flint, L. Smith, A. Haces, D. Minond, S.P. Roche, Eur. J. Med. Chem. 106 (2015) 167–179.
[4] N.P. Kumar, P. Sharma, T.S. Reddy, N. Shankaraiah, S.K. Bhargava, A. Kamal, Eur. J. Med. Chem. 151 (2018) 173–185.
[5] B.B. Toure, D.G. Hall, Chem. Rev. 109 (2009) 4439–4486.
[6] Y.L. Gu, Green Chem. 14 (2012) 2091–2128.
[7] A. Mondal, M. Brown, C. Mukhopadhyay, RSC Adv. 4 (2014) 36890–36895.
[8] V.A. Chebanov, V.F. Saraev, S.M. Desenko, V.N. Chernenko, S.V. Shishkina, O.V. Shishkin, K.M. Kobzar, C.O. Kappe, Org. Lett. 9 (2007) 1691–1694.
[9] V.A. Chebanov, V.F. Saraev, S.M. Desenko, V.N. Chernenko, I.V. Knyazeva, U. Groth, T.N. Glasnov, C.O. Kappe, J. Org. Chem. 73 (2008) 5110–5118.
[10] J. Quiroga, J. Portilla, H. Serrano, R. Abonía, B. Insuasty, M. Nogueras, J. Cobo Tetrahedron Lett. 48 (2007) 1987–1990.
[11] N.K. Terrett, A.S. Bell, D. Brown, P. Ellis, Bioorg. Med. Chem. Lett. 6 (1996) 1819–1824.
[12] T.D. Penning, J.J. Talley, S.R. Bertenshaw, J.S. Carter, P.W. Collins, S. Docter, M.J. Graneto, L.F. Lee, J.W. Malecha, J.M. Miyashiro, R.S. Rogers, D.J. Rogier, S.S. Yu, G.D. Anderson, E.G. Burton, J.N. Cogburn, S.A. Gregory, C.M. Koboldt, W.E. Perkins, K. Seibert, A.W. Veenhuizen, Y.Y. Zhang, P.C. Isakson, J. Med. Chem. 40 (1997) 1347–1365.
[13] S.K. Singh, P.G. Rebby, K.S. Rao, B.B. Lohray, P. Misra, S.A. Rajjak, Y.K. Rao, A. Venkateswarlu, Bioorg. Med. Chem. Lett. 14 (2004) 499–504.
[14] D. Anand, P.K. Yadav, O.P.S. Patel, et al., J. Med. Chem. 60 (2017) 1041–1059.
[15] S.M. Roopan, A. Bharathi, J. Palaniraja, K. Anand, R.M. Gengan, RSC Adv. 48 (2015) 38640–38645.
[16] N.Y. Gorobets, Y.V. Sedash, K.S. Ostras, et al., Tetrahedron Lett. 51 (2010) 2095–2098.
[17] D.Q. Shia, F. Yang, J. Heterocycl. Chem. 48 (2011) 308–311.
[18] K. Karnakar, S.N. Murthy, K. Ramesh, G. Satish, J.B. Nanubolu, Y.V.D. Nageswar, Tetrahedron Lett. 53 (2012) 2897–2903.
[19] D. Bhattacharjee, B. Kshair, B. Myrboh, RSC Adv. 6 (2016) 95944–95950.
[20] C. SYao, C.H. Wang, B. Jiang, S.J. Tu, J. Comb. Chem. 12 (4) (2010) 472–475.
[21] H.Y. Wang, D.Q. Shi, J. Heterocycl. Chem. 49 (2012) 212–216.

[22] H.R. Shaterian, S. Noura, RSC Adv. 4 (2014) 60543–60547.
[23] S.S. Jin, H. Wang, H.Y. Guo, Tetrahedron Lett. 54 (2013) 2353–2356.
[24] M.R. Mousavi, M.T. Maghsoodlou, S.M. Habibi-Khorassani, Mol Divers. 18 (2014) 821–828.
[25] A. Tzani, A. Douka, A. Papadopoulos, E.A. Pavlatou, E. Voutsas, A. Detsi, ACS Sust. Chem. Eng. 1 (2013) 1180–1185.
[26] X. Shi, M. Ding, C. Li, W. Wang, H. Guo, J. Heterocyclic Chem. 55 (2018) 440–446.
[27] L.Q. Kang, Z.J. Cao, Z.J. Lei, Monatsh Chem. 147 (2016) 1125–1128.
[28] S. Sobhani, M. Honarmand, Catal. Lett. 143 (2013) 476–485.
[29] Z. Zhou, J. Yuan, R. Yang, Synt. Commun. 39 (2009) 2001–2007.
[30] S. Sobhani, M. Honarmand, R. Nasseri, Canad. J. Chem. 90 (2012) 798–804.
[31] H. Meng, C.T. Ge, N.N. Ren, W.Y. Ma, Y.Z. Lu, C.X. Li, Ind. Eng. Chem. Res. 53 (2014) 355–362.
[32] M. Waichigo, T. Riechel, N. Danielson, Chromatographia 61 (2005) 17–23.
[33] A.A. Papadopoulou, A. Tzani, D. Alivertis, M.H. Katsoura, A.C. Polydera, A. Detsi, H. Stamatis, Green Chem. 18 (2016) 1147–1158.
[34] (a) M.G. Sharma, R.M. Vala, D.M. Patel, I. Lagunes, M.X. Fernandes, J.M. Padrón, V. Ramkumar, R.L. Gardas, H.M. Patel, Chem. Select. 43 (2018) 12163–12168;
(b) M.G. Sharma, D.P. Rajani, H.M. Patel, R. Soc, Open sci. 4 (2017) 170006;
(c) H.M. Patel, Green Sust. Chem. 5 (2015) 137;
(d) H.M. Patel, K.D. Patel, H.D. Patel, Curr. Bioact. Compd. 13 (2017) 47–58;
(e) H.M. Patel, Curr. Bioact. Compd. 14 (2018) 278–288;
(f) H.M. Patel, D.P. Rajani, M.G. Sharma, H.G. Bhatt, Lett. Drug Des. Discov. 16 (2018) 119–126.
[35] A. Altomare, G. Cascarano, C. Giacovazzo, A. Guagliardi, M.C. Burla, G. Polidori, M. Camalli, J. Appl. Crystallogr. 27 (1994) 435–436.
[36] Crystal Structure Analysis Package, Rigaku Corporation Tokyo (2000–2010) 196-8666, Japan.
[37] G.M. Sheldrick, A short history of SHELX, Acta Crystallogr., A 64 (2008) 112–122.
[38] X.L. Yuan, S.J. Zhang, X.M. Lu, J. Chem. Eng. Data 52 (2007) 596–599.
[39] V.H. Alvarez, S. Mattedi, M. Aznar, J. Chem. Thermodyn. 43 (2011) 895–900.
[40] NCCLS (National Committee for Clinical Laboratory Standards) Twelfth Information Supplement, ISBN 1-56238-454-6 M100-S12 (M7), 2002.
[41] H. Elshaflu, T.R. Todorović, M. Nikolić, A. Lolić, A. Višnjevac, S. Hagenow, J.M. Padrón, A.T. García-Sosa, I.S. Djordjević, S. Grubišić, H. Stark, N.R. Filipović, Front. Chem. 6 (2018) 247.
[42] M. Honarmand, A. Tzani, A. Detsi, J. Iran Chem. Soc. (2018), https://doi.org/10.1007/s13738-018-1537-2.